PCCP

RSC Publishing

PAPER

View Article Online
View Journal | View Issue

Published on 19 October 2012. Downloaded by Ruhr Universitat Bochum on 1/16/2019 10:23:31 AM.

Cite this: *Phys. Chem. Chem. Phys.*, 2013, **15**, 6623

Benchmarks for 0–0 transitions of aromatic organic molecules: DFT/B3LYP, ADC(2), CC2, SOS-CC2 and SCS-CC2 compared to high-resolution gas-phase data†

Nina O. C. Winter,*[a] Nora K. Graf,[a] Samuel Leutwyler[b] and Christof Hättig[a]

Received 2nd August 2012,
Accepted 11th October 2012

DOI: 10.1039/c2cp42694c

www.rsc.org/pccp

In the present study a benchmark set of medium-sized and large aromatic organic molecules with 10–78 atoms is presented. For this test set 0–0 transition energies measured in supersonic jets are compared to those calculated with DFT and the B3LYP functional, ADC(2), CC2 and the spin-scaled CC2 variants SOS-CC2 and SCS-CC2. Geometries of the ground and excited states have been optimized with these methods in polarized triple zeta basis sets. Zero-point vibrational corrections have been calculated with the same methods and basis sets. In addition the energies have been corrected by single point calculations with a triple zeta basis augmented with diffuse functions, aug-cc-pVTZ. The deviations of the theoretical results from experimental electronic origins, which have all been measured in the gas phase with high-resolution techniques, were evaluated. The accuracy of SOS-CC2 is comparable to that of unscaled CC2, whereas ADC(2) has slightly larger errors. The lowest errors were found for SCS-CC2. All correlated wave function methods provide significantly better results than DFT with the B3LYP functional. The effects of the energy corrections from the augmented basis set and the method-consistent calculation of the zero-point vibrational corrections are small. With this benchmark set reliable reference data for 0–0 transition energies for larger organic chromophores are available that can be used to benchmark the accuracy of other quantum chemical methods such as new DFT functionals or semi-empirical methods for excitation energies and structures and thereby augments available benchmark sets augments present benchmark sets which include mainly smaller molecules.

1 Introduction

The description of electronically excited states is a demanding task of quantum chemistry. Multireference methods such as the complete active space perturbation theory of second order, CASPT2, or multireference configuration interaction, MRCI, can describe electronically excited states with a high accuracy. These methods are still applicable in cases where already the ground state shows near-degenerate effects. Unfortunately multi-reference methods are computationally very expensive so that they can only be applied to small molecules with small basis sets. For larger molecules single reference methods have to be used, which describe excited states within response theory.

A widely used single reference model for the description of excited states that describes dynamic electron correlation up to second order perturbation theory is the approximate coupled cluster model CC2.[1] The CC2 model is known to predict excitation energies with deviations of less than 0.3 eV[2–4] from experimental or highly accurate calculated reference results if the electronic structure of the excited state is dominated by single excitations out of the ground state. Another correlated single reference method is the algebraic diagrammatic construction through second order, ADC(2),[5] which is known to provide a similar accuracy for the description of excited states to CC2. The ADC(2) model can be seen as an approximation to CC2 where the cluster amplitudes of the ground state singles are neglected.[6] Due to the neglect of these single contributions ADC(2) covers slightly less correlation effects than CC2.

During the last few years spin-scaled methods were discovered as efficient tools in the field of quantum chemistry. Spin-component scaled SCS-MP2[7] and the related SCS-CIS(D) for the description of excited states[8] are known to predict better results than the unscaled methods without increasing the computational costs. In addition a scaled opposite-spin (SOS) ansatz for MP2[9] and CIS(D)[10] was proposed, which provides about the same accuracy as the unscaled methods but can be implemented with reduced computational costs for large molecules.[9–12] These spin-scaled ideas have also been applied to the CC2 method with promising results.[13–15]

Unfortunately correlated single reference methods are still too expensive to be applied to large molecules with hundreds of atoms.

[a] *Lehrstuhl für Theoretische Chemie, Ruhr-Universität Bochum, D-44780 Bochum, Germany. E-mail: Nina.Winter@theochem.rub.de, Nora.Graf@rub.de, Christof.Haettig@rub.de*

[b] *Departement für Chemie und Biochemie, University of Bern, Freiestrasse 3, CH-3012 Bern, Switzerland. E-mail: leutwyler@iac.unibe.ch*

† Electronic supplementary information (ESI) available: 0–0 Transition energies, zero-point vibrational corrections and molecular structures. See DOI: 10.1039/c2cp42694c

Published on 19 October 2012. Downloaded by Ruhr Universitat Bochum on 1/16/2019 10:23:31 AM.

In such cases density functional theory (DFT) methods have to be used. But DFT with standard exchange correlation functionals like *e.g.* B3LYP[16] faces problems for the description of certain electronically excited states. One main problem is the fact that usual hybrid functionals fail for the description of charge transfer excited states.[17] Therefore the development of new DFT functionals or semi-empirical methods with low computational costs is of interest to describe excited states of large molecules. The accuracy of these new methods has to be benchmarked using large test sets with reliable reference results.

There are already several test sets for excitation energies available.[18] But the accuracy of such benchmark sets is usually limited by certain facts. When calculated data from high-level methods are used as a reference,[4,19,20] the comparison is limited by the accuracy of the reference method. Thus accurate experimental reference data are desirable, which can directly be compared to theoretical results. Several benchmark studies use experimental reference data and compare it with calculated vertical excitation energies.[21–24] The accuracy of such studies is always limited by the neglect of vibrational contributions. If theoretical 0–0 transitions are considered the comparison still suffers from a solvent shift when the measurements are not carried out in the gas phase.[8,25] To perform accurate benchmark studies 0–0 transitions should be calculated and compared with high-resolution gas-phase data. This has been done *e.g.* in ref. 26 for a test set of 91 molecules including organic molecules, radicals and transition metal compounds. But most of the included organic molecules are relatively small. The current work extends the available benchmark sets for 0–0 transition energies towards larger organic chromophores. In addition we include several conformers for some of the molecules to provide a test for the accuracy with which electronic structure methods reproduce the tiny excitation energy differences between such structures.

In the present study we present a compilation of 66 band origins for organic molecules, which have all been measured in supersonic jets with high-resolution techniques. Six of these molecules are also part of the test set presented in ref. 26 but were not included in the reduced set to test CC2 and ADC(2). All molecules of this benchmark set can be described by single reference ground states so that they can be used to assess the accuracy of correlated single-reference wavefunction methods. For this test set we calculated 0–0 transition energies with DFT and the B3LYP functional, ADC(2), CC2, SCS-CC2 and SOS-CC2. These calculated data can directly be compared with the experimental gas phase results and thereby provide together with existing benchmark sets for smaller molecules a reliable reference for future developments of electronic structure methods for the description of excited states also of larger organic closed-shell molecules.

2 Computational details

Benchmark calculations with DFT/B3LYP, ADC(2), CC2, SOS-CC2 and SCS-CC2 have been carried out for a set of 66 organic molecules such as porphine derivatives, polycyclic aromatic hydrocarbons, heterocyclic organic compounds and aromatic alcohols. The geometries of the chromophores were optimized in the ground and first excited singlet state with all methods. Based on the obtained equilibrium structures zero-point vibrational corrections in the harmonic approximation were calculated with the same methods. For the DFT/B3LYP calculations we applied the basis set TZVP[27] whereas the basis set TZVPP[28] was used for the correlated wavefunction based methods because the latter shows a slower convergence with the basis set size. Finally single point calculations with the aug-cc-pVTZ[29,30] basis set were carried out with all methods at the corresponding TZVPP/TZVP equilibrium structures. From these results corrections for diffuse functions were obtained as difference between the electronic energies with TZVPP/TZVP and aug-cc-pVTZ.

Due to the large computational effort for tetraphenylporphine (TPP) and zinc tetraphenylporphine (Zn-TPP) no method-consistent zero-point correction could be calculated. For these two molecules the 0–0 transitions with zero-point corrections from DFT/B3LYP are given instead.

All calculations have been carried out with the program package TURBOMOLE.[31] For the DFT/B3LYP calculations the modules escf[32] and egrad[33] have been used to calculate excited state energies and gradients. For ADC(2), CC2, SOS-CC2 and SCS-CC2 the resolution-of-the-identity (RI) approximation with corresponding auxiliary basis sets[28,34] and the frozen-core approximation have been applied. For SCS-CC2 and SOS-CC2 the spin scaling factors from ref. 13 were used. The second derivatives for the calculation of the vibrational corrections were obtained by numerical derivation of the analytical gradients for all correlated wave function methods and for DFT/B3LYP in the case of excited states. Analytical second derivatives were used only for DFT calculations on ground states.

3 Results and discussion

3.1 Assignment of experimental data

The benchmark set contains 66 organic structures. Some of these structures are different conformational isomers of the same chromophore. To compare the computed 0–0 transitions with the experimental bands the experimental data have to be assigned to the individual isomeric structures.

For some of the considered molecules these assignments were already available from the original publications. The experimental bands of tryptamine are clearly assigned to six different isomers in ref. 35. For the nomenclature of these isomers we refer also to ref. 35. Catechol can form three isomers, which differ by the position of the hydroxyl groups. But in ref. 36 only one experimental band is reported. This band is assigned to the most stable isomer with an intramolecular hydrogen bond,[36] which is depicted in Fig. 1.

For some other molecules of the benchmark set no clear assignment of the experimental bands was available. The experimental transitions of these molecules were assigned based on our calculated data. These assignments are described in the following paragraphs.

Tetraphenylporphine (TPP) and zinc tetraphenylporphine (Zn-TPP) can form four different isomers depending on the orientation of the four phenyl groups with respect to the porphine ring. The isomers of Zn-TPP are depicted in Fig. 2. The four isomers of TPP can be constructed in the same way as for Zn-TPP, where the numbering of the TPP isomers follows the same scheme as in Fig. 2.

The experimental data reproduce only one electronic band for TPP and Zn-TPP, respectively, that belongs to the most stable isomer in each case.[37] To determine the most stable structures of TPP and Zn-TPP we carried out DFT/B3LYP calculations with the TZVP basis set for all isomers. In the ground state the individual isomers of TPP

 This journal is © the Owner Societies 2013

Published on 19 October 2012. Downloaded by Ruhr Universitat Bochum on 1/16/2019 10:23:31 AM.

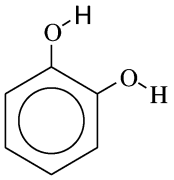


Fig. 1 Isomer of catechol which is assigned to the experimental band in ref. 36.

and Zn-TPP are separated by less than 1 kJ mol^{-1} and for both molecules isomer 1 has the lowest ground state energy.

The results for 0–0 transition energies, which were calculated with DFT/B3LYP and the TZVP basis set for all isomers of TPP and Zn-TPP, are given in Table 1. During the geometry optimization in the first excited state isomer 3 of Zn-TPP converts into isomer 1. The optimized structure of isomer 2 of Zn-TPP in the excited state shows an imaginary vibrational frequency within the harmonic approximation and is thereby identified as a transition state. For isomers 1 and 4 of Zn-TPP a stable equilibrium structure in the excited state could be obtained. Isomer 1 has the lowest 0–0 transition energy. The 0–0 transition energy for isomer 4 is only 0.007 eV larger than for isomer 1.

For TPP we found four minima on the potential energy surface of the excited state. Isomer 1 has the lowest 0–0 transition energy. The 0–0 transition energies of the other three isomers are less than 0.007 eV higher than the one of isomer 1. Thus the isomeric shifts of the 0–0 transition energies of both TPP and Zn-TPP are very small. We carried out the calculations for the correlated wave function methods only for isomer 1 of TPP and Zn-TPP, which has the lowest energy in the ground and excited state with DFT/B3LYP.

Resorcinol can form three isomers which are depicted in Fig. 3. According to ref. 38 three bands are measured for resorcinol.

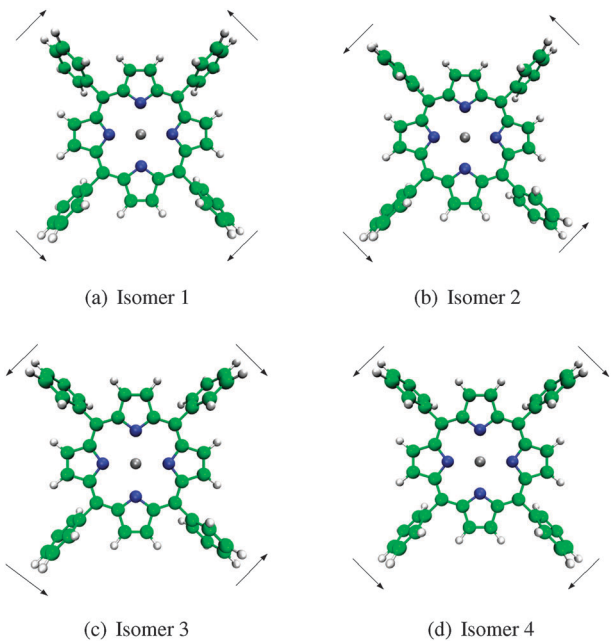


Fig. 2 Four conformational isomers of zinc tetraphenylporphine (Zn-TPP). The arrows indicate the direction of rotation of the phenyl groups with respect to the porphine molecular plane. For the benchmark calculations isomer 1 was used, which has the lowest ground state energy and the lowest 0–0 transition energy with DFT/B3LYP/TZVP.

Table 1 0–0 Transition energies of tetraphenylporphine (TPP) and zinc tetraphenylporphine (Zn-TPP) calculated with DFT/B3LYP and the basis set TZVP

	TPP	Zn-TPP
Isomer 1	2.013	2.186
Isomer 2	2.077	2.192[a]
Isomer 3	2.066	—[b]
Isomer 4	2.069	2.193

[a] Not an equilibrium structure in the excited state. [b] Not stable under structure relaxation in the excited state.

In ref. 38 the band at 4.486 eV is assigned to isomer 1 due to the intensity of the transition whereas the bands at 4.455 eV and 4.483 eV were not assigned. To connect also the isomers 2 and 3 to experimental bands we considered our SCS-CC2 results. SCS-CC2 provides the highest accuracy of all methods in this study. With SCS-CC2 we obtained the lowest 0–0 transition energy of 4.422 eV for isomer 3. In agreement with the experimental data the transition energies for isomer 2 and isomer 1 are about 0.03 eV higher than for isomer 3. Therefore the isomers of resorcinol can clearly be assigned to the measured bands according to Table 2.

Methoxyphenol can form four conformational isomers when the substituents are at the *ortho* or *meta* position to each other. In ref. 39 only one experimental band is given for *ortho*-methoxyphenol, which is assigned to the isomer from Fig. 4 with an intramolecular hydrogen bond. Due to the analysis of the vibronic band structure the hydrogen bound isomer is the only one present in the supersonic jet.[39]

For *meta*-methoxyphenol two experimental bands are given in ref. 39, which were not unambiguously assigned to one of the isomers. The structures of the four isomers of *meta*-methoxyphenol are depicted in Fig. 5. Ref. 39 suggests to assign the experimental bands to isomers 1 and 4, which are the most stable ones in the ground state. To check this assumption we considered again our SCS-CC2 results. Based on the vibrationally corrected SCS-CC2 ground state energies the isomers 1 and 4 are indeed lower in energy than the isomers 2 and 3 but the energy difference is below 2 kJ mol^{-1}. Therefore one has to assume that all four isomeric structures of *meta*-methoxyphenol are populated in the ground state.

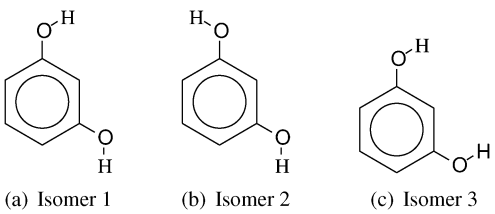


Fig. 3 Isomers of resorcinol.

Table 2 0–0 Transition energies for the isomers of resorcinol calculated with SCS-CC2 and TZVPP with corrections for diffuse functions from the basis set aug-cc-pVTZ

	SCS-CC2	Exp.
Isomer 2	4.4553	4.4828[a]
Isomer 1	4.4568	4.4860[a]
Isomer 3	4.4221	4.4551[a]

[a] Exp. data from ref. 38.

Published on 19 October 2012. Downloaded by Ruhr Universitat Bochum on 1/16/2019 10:23:31 AM.

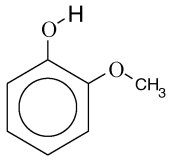


Fig. 4 Isomer of *ortho*-methoxyphenol which is assigned to the experimental band in ref. 39.

In the following we assign the experimental bands of *meta*-methoxyphenol according to the SCS-CC2 0–0 transition energies, which were obtained in this study. SCS-CC2 predicts the lowest transition energy of 4.418 eV for isomer 2. The transition energy for isomer 4 of 4.425 eV is slightly larger than for isomer 2. Therefore we assign the isomers 2 and 4, respectively, to the experimental bands with transition energies of 4.459 eV and 4.467 eV.

For *para*-methoxyphenol two experimental bands are given in ref. 39 and again no clear assignment to the two conformational isomers is provided. For *para*-methoxyphenol we applied the same strategy as for *meta*-methoxyphenol and assigned the experimental bands based on the SCS-CC2/TZVPP calculations. The SCS-CC2 excitation energy for the *trans* isomer is by 0.014 eV larger than for the *cis* isomer, which fits to the experimental difference in excitation energies of 0.012 eV. Therefore, the experimental band at 4.1609 eV is assigned to the *trans* isomer and the band at 4.1729 eV to the *cis* isomer.

The nomenclature of the excited states is based on the molecular symmetry, which is obtained in the excited state geometry optimizations. For some molecules the symmetry of the equilibrium structures changes under optimization with another quantum chemical method. In these cases the nomenclature of the excited states follows the highest molecular symmetry that could be found with one of the methods.

To assign the excited states to an irreducible representation the conventions from ref. 40 are used. For Zn-TPP and tetrafluorobenzene these conventions are not applicable because these molecules have C_{2v} symmetry in the excited state but are not planar. In these cases the axis of rotation is perpendicular to the molecular layer and is chosen as the z axis. For tetrafluorobenzene both hydrogens are located on the y axis. The choice of the x and y axis for Zn-TPP is illustrated in Fig. 6. For all molecules the lowest excited singlet state was considered. All transitions have ππ* character with the exception of the $^1A''$ states of 2-methylpyrimidine and 5-methylpyrimidine and the excited state of pyrazine, which have nπ* character.

The keto isomer of 2-hydroxyquinoline was optimized in the excited state with C_s symmetry. The resultant structures, which were obtained with DFT/B3LYP and CC2, were identified as transition states. When the geometry was optimized with the same methods without symmetry constraints only equilibrium structures for a nπ* state could be obtained. This state is the second excited state of the vertical excitation spectrum and does not correspond to the experimental transition. We report therefore the results with C_s symmetry for all methods.

The optimizations of catechol in the excited state were carried out without symmetry constraints. DFT/B3LYP predicts a first excited state with πσ* character during the optimization. The resulting structure with DFT/B3LYP has an unusually large O–H distance and the corresponding geometry optimizations could not be converged.

3.2 Statistical analysis

The 0–0 transition energies for the benchmark set calculated with DFT/B3LYP, ADC(2), CC2, SCS-CC2 and SOS-CC2 are listed in Table 3. The statistical analysis of the results is given in Table 4 and the error distributions are shown in Fig. 7.

The mean errors are nearly zero for all methods. Among the methods studied in this work DFT with B3LYP has the largest maximum error, mean absolute error and the largest standard deviation. The maximum error of 0.75 eV occurs for decatetraene whose molecular structure is similar to octatetraene for which B3LYP leads as well to errors of about 0.7 eV.[8,13]

All correlated wave function methods lead to significantly smaller errors than B3LYP. For the CC2 methods the maximum error for this test set is lower than 0.30 eV, the standard deviation is lower than 0.10 eV and the mean absolute error is at most 0.07 eV. The errors for SOS-CC2 are slightly lower than for unscaled CC2. SCS-CC2 has the lowest errors of all methods with a maximum error, a mean absolute error and a standard deviation of 0.13 eV, 0.05 eV and 0.06 eV, respectively.

The errors for ADC(2) are slightly larger than for the CC2 methods. The reason for this is the fact that ADC(2) covers slightly less correlation effects than the CC2 methods due to the neglect of the single ground state amplitudes in the ADC(2) method. The maximum error of ADC(2) of 0.38 eV occurs for the ππ* state of 2-pyridone. In this case unscaled CC2 predicts a comparatively high D1 diagnostics[71] of 0.13 for the equilibrium structure of the excited state, which indicates a non-negligible contribution of singly excited determinants to the

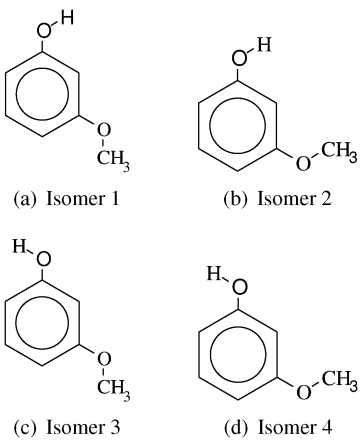


Fig. 5 Isomers of *meta*-methoxyphenol.

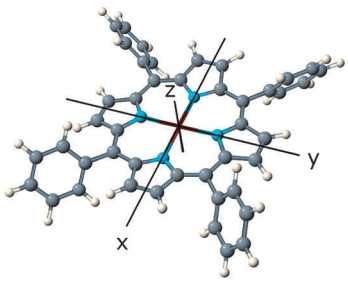


Fig. 6 Structure of zinc tetraphenylporphine with the positions of the axes.

 This journal is © the Owner Societies 2013

Published on 19 October 2012. Downloaded by Ruhr Universitat Bochum on 1/16/2019 10:23:31 AM.

Table 3 0–0 Transition energies in eV calculated with DFT/B3LYP, ADC(2), CC2, SCS-CC2 and SOS-CC2. The equilibrium structures and zero-point vibrational corrections were obtained with the TZVP basis set in the case of DFT/B3LYP and with the TZVPP basis set for all other methods. In addition corrections for diffuse functions from single point calculations with the basis set aug-cc-pVTZ were applied. Experimental reference data from high-resolution gas-phase measurements with vacuum corrections are given for comparison. The given symmetries refer to the excited state structures and in each case the lowest excited state in the given irreducible representation was calculated

Molecule	Symmetry	B3LYP	ADC(2)	CC2	SCS-CC2	SOS-CC2	Exp.	Ref.
Tetraphenylporphine	C_2, ^{1}B	2.006	1.931[a]	1.991[a]	1.896[a]	1.829[a]	1.9400	37
Zn-tetraphenylporphine	C_{2v}, $^1B_1$	2.182	2.140[a]	2.207[a]	2.168[a]	2.114[a]	2.1679	37
Porphycene	C_s, $^1A'$	2.105	1.718	2.038	1.985	1.986	2.0049	41
Porphine	D_{2h}, $^1B_{1u}$	2.215	2.087	2.204	2.093	2.044	2.0229	42
Chlorin	C_{2v}, $^1B_2$	2.236	1.966	2.108	2.016	1.971	1.9723	43
Tetracene	D_{2h}, $^1B_{1u}$	2.136	2.506	2.551	2.745	2.840	2.7753	44
Perylene	C_2, ^{1}B	2.578	2.724	2.771	2.939	3.032	2.9830	45
Phenanthrene	C_{2v}, $^1A_1$	3.702	3.758	3.727	3.722	3.722	3.6360	46
Fluorene	C_{2v}, $^1B_1$	4.155	4.238	4.211	4.189	4.166	4.1865	47
Carbazole	C_{2v}, $^1A_1$	3.749	3.789	3.803	3.848	3.865	3.8186	47
Dibenzofuran	C_{2v}, $^1A_1$	4.133	3.997	4.037	4.045	4.044	4.1702	47
Pyrrolo[3,2-*h*]quinoline	C_s, $^1A'$	3.457	3.654	3.649	3.714	3.731	3.6595	48
Tryptamine								
A-ph[b,i]	C_1, ^{1}A	4.080	4.279	4.288	4.427	4.321	4.3232	35, 49
A-py[c,i]	C_1, ^{1}A	4.059	4.262	4.271	4.415	4.323	4.3239	35, 49
A-up[d,i]	C_1, ^{1}A	4.013	4.256	4.263	4.413	4.322	4.3219	35, 49
Ph-out[e,i]	C_1, ^{1}A	4.078	4.286	4.299	4.437	4.325	4.3239	35, 49
Ph-up[f,i]	C_1, ^{1}A	3.970	4.236	4.243	4.395	4.318	4.3173	35, 49
Py-out[g,i]	C_1, ^{1}A	4.064	4.267	4.280	4.420	4.325	4.3277	35, 49
Py-up[h,i]	C_1, ^{1}A	4.047	4.286	4.296	4.422	4.323	4.3252	35, 49
2,4,6,8-Decatetraene	C_{2h}, ^1B_u	3.562	3.956	4.020	4.232	4.340	4.3115	50
5-MO-salicylic acid[j]	C_s, $^1A'$	3.351	3.248	3.328	3.491	3.551	3.4893	51
Salicylic acid	C_s, $^1A'$	3.737	3.366	3.535	3.699	3.838	3.6951	51
3P-1-propionic acid[k], *gauche*	C_1, ^{1}A	5.001	4.823	4.800	4.654	4.586	4.6666	52
3P-1-propionic acid[k], *anti*	C_s, $^1A''$	5.003	4.817	4.788	4.648	4.586	4.6638	52
1-Naphthol, *cis*	C_1, ^{1}A	3.612	3.856	3.889	3.908	3.883	3.8659	53
1-Naphthol, *trans*	C_s, $^1A'$	3.729	3.960	3.986	3.958	3.932	3.9000	53
2-Naphthol, *cis*	C_s, $^1A'$	3.770	3.876	3.885	3.885	3.876	3.8304	54
2-Naphthol, *trans*	C_s, $^1A'$	3.706	3.782	3.787	3.808	3.805	3.7912	54
7-Hydroxyquinoline, *cis*	C_s, $^1A'$	3.731	3.802	3.824	3.857	3.858	3.8230	55
7-Hydroxyquinoline, *trans*	C_1, ^{1}A	3.517	3.750	3.782	3.823	3.833	3.7830	55
2-Hydroxyquinoline, enol	C_s, $^1A'$	3.815	3.856	3.882	3.904	3.899	3.8857	56
2-Hydroxyquinoline, keto	C_s, $^1A'$	3.600	3.490	3.522	3.653	3.708	3.6084	56
m-Dimethoxybenzene[l], *trans*	C_s, $^1A'$	4.555	4.365	4.409	4.402	4.358	4.4313	57
7-Azaindole	C_s, $^1A'$	4.053	4.231	4.245	4.348	4.274	4.2929	58
Phenylacetylene	C_{2v}, $^1B_2$	4.695	4.521	4.605	4.516	4.470	4.4469	59
Benzonitrile	C_{2v}, $^1B_2$	4.823	4.729	4.694	4.592	4.513	4.5257	60
Aniline	C_s, $^1A''$	4.274	4.231	4.234	4.228	4.208	4.2180	61
Tetrafluorobenzene	C_{2v}, $^1B_1$	4.668	4.511	4.528	4.508	4.478	4.5309	62
2,6-Difluoropyridine	C_{2v}, $^1B_2$	4.957	4.730	4.715	4.648	4.606	4.6877	63
2-Fluoropyridine	C_s, $^1A'$	4.585	4.782	4.771	4.681	4.632	4.7124	64
2-Hydroxypyridine	C_s, $^1A'$	4.677	4.476	4.488	4.448	4.418	4.4774	65
2-Methylpyrimidine	C_s, $^1A''$	3.587	3.571	3.645	3.873	3.989	3.7754	66
5-Methylpyrimidine	C_s, $^1A''$	3.625	3.651	3.697	3.924	4.034	3.8177	66
Pyrazine[m]	C_{2h}, ^1B_u	3.581	3.823	3.794	3.958	4.077	3.8271	67
2-Pyridone	C_s, $^1A'$	3.846	3.323	3.565	3.715	3.778	3.6986	68
Catechol	C_1, ^{1}A	—[n]	4.438	4.444	4.424	4.387	4.4187	36
Resorcinol, isomer 2	C_{2v}, $^1B_2$	4.741	4.548	4.520	4.455	4.420	4.4828	38
Resorcinol, isomer 1	C_1, ^{1}A	4.692	4.527	4.541	4.457	4.405	4.4860	38

Published on 19 October 2012. Downloaded by Ruhr Universitat Bochum on 1/16/2019 10:23:31 AM.

Table 3 (*continued*)

Molecule	Symmetry	B3LYP	ADC(2)	CC2	SCS-CC2	SOS-CC2	Exp.	Ref.
Resorcinol, isomer 3	C_s, $^1A''$	4.592	4.461	4.466	4.422	4.386	4.4551	38
Hydroquinone, *cis*	C_{2v}, $^1A_1$	4.243	4.093	4.107	4.105	4.094	4.1564[o]	38
Hydroquinone, *trans*	C_{2h}, ^1B_u	4.258	4.132	4.142	4.148	4.136	4.1522[o]	38
o-Methoxyphenol	C_1, ^1A	4.576	4.439	4.462	4.423	4.362	4.4509	39
m-Methoxyphenol, isomer 4	C_1, ^1A	4.697	4.493	4.516	4.425	4.398	4.4665	39
m-Methoxyphenol, isomer 2	C_1, ^1A	4.610	4.448	4.463	4.418	4.380	4.4589	39
p-Methoxyphenol, *trans*	C_1, ^1A	4.230	4.065	4.090	4.096	4.087	4.1609	39
p-Methoxyphenol, *cis*	C_1, ^1A	4.242	4.082	4.098	4.110	4.101	4.1729	39
o-Fluorophenol, *cis*	C_1, ^1A	4.704	4.621	4.622	4.541	4.494	4.5618	39
o-Fluorophenol, *trans*	C_1, ^1A	4.700	4.585	4.594	4.527	4.473	4.5751	39
m-Fluorophenol, *cis*	C_1, ^1A	4.785	4.622	4.629	4.536	4.474	4.5394	39
m-Fluorophenol, *trans*	C_s, $^1A'$	4.824	4.624	4.629	4.543	4.500	4.5650	39
p-Fluorophenol	C_s, $^1A'$	4.540	4.332	4.346	4.315	4.288	4.3526	39
o-Cresol, *cis*	C_1, ^1A	4.675	4.585	4.582	4.504	4.455	4.5143	69
o-Cresol, *trans*	C_1, ^1A	4.667	4.542	4.555	4.453	4.419	4.4876	69
m-Cresol, *cis*	C_1, ^1A	4.661	4.504	4.511	4.428	4.388	4.4608	69
m-Cresol, *trans*	C_s, $^1A'$	4.722	4.566	4.566	4.491	4.446	4.4743	69
p-Cresol	C_1, ^1A	4.556	4.413	4.335	4.317	4.443	4.3790	69

[a] Zero-point vibrational corrections taken from DFT/B3LYP calculations. [b] *Anti*-ph. [c] *Anti*-py. [d] *Anti*-up. [e] *gauche*-Phenyl-out. [f] *gauche*-Phenyl-up. [g] *gauche*-Pyrrole-out. [h] *gauche*-Pyrrole-up. [i] Nomenclature taken from ref. 49. [j] 5-Methoxysalicylic acid. [k] 3-Phenyl-1-propionic acid. [l] Symmetry with SOS-CC2: C_2, ^1A. [m] Symmetry with CC2 and ADC(2): C_1, ^1A_u; symmetry with B3LYP: C_{2h}, ^1A_u. [n] B3LYP predicts S_1 state with $\pi\sigma^*$ character. [o] Assignment to the isomers taken from ref. 70.

Table 4 Statistical evaluation of the errors for the 0–0 transitions from Table 3. The maximum absolute error (MAX), mean error (ME), mean absolute error (MAE) and the standard deviation (SD) are listed in eV. The standard deviation s is given as $s = \sqrt{\frac{\sum_i^n (x_i - \bar{x})^2}{n-1}}$ where $\bar{x}$ is the mean error and n is the number of excited states

	B3LYP	ADC(2)	CC2	SCS-CC2	SOS-CC2
MAX	0.75	0.38	0.29	0.13	0.25
ME	0.00	−0.03	0.00	0.01	−0.01
MAE	0.19	0.08	0.07	0.05	0.06
SD	0.23	0.12	0.09	0.06	0.08

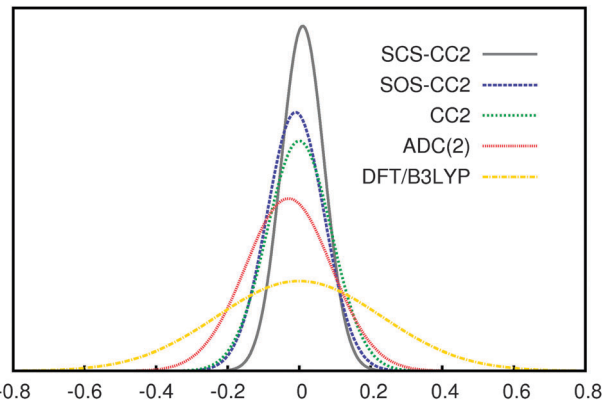


Fig. 7 Error distribution for the 0–0 transitions in eV.

ground state wave function at this geometry. Experimental results predict a non-planar equilibrium structure for the ππ* state of 2-pyridone.[68] This non-planarity of the excited state structure of 2-pyridone is correctly described by CASSCF calculations,[72] whereas the present calculations resulted in planar equilibrium structures with all methods. Thus the large error of ADC(2) for the ππ* state of 2-pyridone is probably due to strong correlation effects in the ground state wave function at the equilibrium geometry of the excited state.

To evaluate the effect of diffuse functions on the basis set 0–0 transition energies were calculated without corrections from single point calculations with the basis set aug-cc-pVTZ. Detailed results are listed in the ESI.† The corresponding statistical analysis is given in Table 5. Without corrections for diffuse functions the mean errors of all methods increase by 0.03–0.05 eV whereas the effect on the mean absolute error and the standard deviation is very small. The inclusion of diffuse functions in the basis set usually leads to a larger stabilization of the excited state so that the excitation energy decreases. The neglect of diffuse functions in the present case leads to a general shift to higher excitation energies so that the mean errors increase whereas the mean absolute errors and the standard deviations are not affected. The maximum errors differ by at most 0.06 eV. For B3LYP, ADC(2) and CC2 the maximum error is negative so that it decreases without corrections for diffuse functions. For SCS-CC2 and SOS-CC2 the maximum error is positive so that it increases when diffuse functions are left out.

Finally the effect of method-consistent vibrational corrections is evaluated. For this 0–0 transition energies were calculated by combining the TZVP/TZVPP energies of each method and zero-point vibrational corrections from the DFT/B3LYP calculations. In the case of catechol the geometry optimization

This journal is © the Owner Societies 2013

Published on 19 October 2012. Downloaded by Ruhr Universitat Bochum on 1/16/2019 10:23:31 AM.

Table 5 Statistical evaluation of the errors for 0–0 transitions obtained without corrections for diffuse functions from the aug-cc-pVTZ basis set. The corresponding 0–0 transition energies are listed in the ESI. All values are given in eV

	B3LYP	ADC(2)	CC2	SCS-CC2	SOS-CC2
MAX	0.72	0.32	0.25	0.19	0.29
ME	0.05	0.01	0.04	0.05	0.03
MAE	0.20	0.08	0.08	0.06	0.06
SD	0.23	0.12	0.09	0.06	0.08

Table 6 Statistical evaluation of the errors for 0–0 transitions obtained without corrections for diffuse functions and with zero-point vibrational corrections from DFT/B3LYP. The corresponding 0–0 transition energies are listed in the ESI. All values are given in eV

	B3LYP	ADC(2)	CC2	SCS-CC2	SOS-CC2
MAX	0.72	0.33	0.27	0.23	0.27
ME	0.05	0.05	0.07	0.07	0.03
MAE	0.20	0.10	0.10	0.07	0.06
SD	0.23	0.12	0.10	0.07	0.08

in the excited state did not converge with B3LYP. In this case we used the zero-point corrections from MP2/ADC(2) instead. The detailed results are listed in the ESI.† The corresponding statistical analysis can be taken from Table 6.

For ADC(2), CC2 and SCS-CC2 the mean errors increase by 0.02–0.04 eV and the mean absolute errors and standard deviations increase by up to 0.02 eV when vibrational corrections from DFT are applied. The mean error, the mean absolute error and the standard deviation of SOS-CC2 are not affected at all by the use of vibrational corrections from DFT. The maximum error increases slightly for ADC(2), CC2 and SCS-CC2 whereas it decreases for SOS-CC2. Altogether the results are affected only slightly when 0–0 transition energies are calculated from zero-point vibrational corrections from DFT/B3LYP. The calculation of vibrational corrections is one of the most time-consuming steps when 0–0 transition energies are of interest. Therefore it would be desirable to obtain these corrections with a lower level method. The results from the present study suggest that the use of vibrational corrections from DFT/B3LYP is sufficient in most cases.

4 Summary and conclusion

We compiled a new benchmark set of 66 aromatic organic closed-shell molecules for which experimental band origins have been measured in the gas phase with high-resolution techniques. This work extends existing benchmark sets, as proposed *e.g.* in ref. 26, for adiabatic or 0–0 transition energies towards larger molecules with up to 78 atoms and it focuses on single-excitation dominated transitions in molecules with single-reference ground states.

We calculated 0–0 transition energies with DFT/B3LYP, ADC(2), CC2, SOS-CC2 and SCS-CC2 for all 66 molecules. The geometries were optimized with each method and a basis set of triple zeta quality. Zero-point vibrational corrections were calculated with the same basis sets and methods. In addition corrections for diffuse functions in the basis set were obtained from single point calculations with aug-cc-pVTZ. The resultant equilibrium structures and zero-point vibrational corrections can be used to obtain 0–0 transition energies with other quantum chemical methods (higher-order wave function methods, new DFT functionals or semi-empirical methods) with comparatively low computational costs. The accuracy of these methods for the description of excited states can thereby be evaluated easily and the comparison with high-resolved gas phase data ensures a very good reliability of the obtained results since uncertainties caused by solvent shifts or empirical corrections for geometry relaxation effects or zero-point vibrational corrections are omitted.

The statistical analysis of the theoretical results from DFT/B3LYP, ADC(2), CC2, SOS-CC2 and SCS-CC2 shows that the mean errors are nearly zero for all considered methods. For the present test set the errors for SOS-CC2 are slightly smaller than for unscaled CC2, whereas ADC(2) leads to slightly larger errors than CC2. The lowest deviations from the experimental values were obtained for SCS-CC2. The correlated wave function methods lead for this test set to significantly better results than DFT with the B3LYP functional. Without corrections for diffuse functions the mean errors increase by up to 0.05 eV whereas the maximum absolute errors, mean absolute errors and the standard deviations are affected only slightly. When zero-point vibrational corrections from the DFT calculations are used instead of method-consistent vibrational corrections the results change only slightly.

SCS-CC2 predicts the smallest errors of all considered methods for 0–0 transition energies of excited states. As the spin-scaling introduces no additional computational costs compared to unscaled CC2, we recommend using SCS-CC2 with basis sets including diffuse function and method-consistent zero-point vibrational corrections to fully exploit the accuracy of second-order wave function based methods. SOS-CC2 provides slightly better results than unscaled CC2 for the present test set and can be implemented with computational costs that scale only with the fourth power of the system size.[14,15] This holds also true for a SOS version of ADC(2). Thus the formal scaling behavior (without considering integral screening) of SOS-CC2 and SOS-ADC(2) is the same as for DFT with hybrid functionals. If one aims at calculating 0–0 transitions of larger aromatic molecules ($\approx$50–150 atoms) with low computational costs one should therefore use SOS-CC2 or SOS-ADC(2) with basis sets of triple zeta quality in combination with zero-point vibrational corrections from DFT/B3LYP.

Acknowledgements

Thanks to Susan Blaser and Patrick Steinegger for compiling the experimental reference data.

References

1 O. Christiansen, H. Koch and P. Jørgensen, *Chem. Phys. Lett.*, 1995, **243**, 409.
2 H. Koch, O. Christiansen, P. Jørgensen and J. Olsen, *Chem. Phys. Lett.*, 1995, **244**, 75–82.
3 O. Christiansen, H. Koch, P. Jørgensen and J. Olsen, *Chem. Phys. Lett.*, 1996, **256**, 185–194.
4 M. Schreiber, M. R. Silva-Junior, S. P. A. Sauer and W. Thiel, *J. Chem. Phys.*, 2008, **128**, 134110.
5 J. Schirmer, *Phys. Rev. A: At., Mol., Opt. Phys.*, 1982, **26**, 2395.
6 C. Hättig, *Adv. Quantum Chem.*, 2005, **50**, 37.
7 S. Grimme, *J. Chem. Phys.*, 2003, **118**, 9095.
8 S. Grimme and E. I. Izgorodina, *Chem. Phys.*, 2004, **305**, 223.

Published on 19 October 2012. Downloaded by Ruhr Universitat Bochum on 1/16/2019 10:23:31 AM.

9 Y. Jung, R. C. Lochan, A. D. Dutoi and M. Head-Gordon, *J. Chem. Phys.*, 2004, **121**, 9793–9802.
10 Y. M. Rhee and M. Head-Gordon, *J. Phys. Chem.*, 2007, **111**, 5314–5326.
11 R. C. Lochan, Y. Shao and M. Head-Gordon, *J. Chem. Theory Comput.*, 2007, **3**, 988–1003.
12 Y. M. Rhee, D. Casanova and M. Head-Gordon, *J. Chem. Theory Comput.*, 2009, **5**, 1224–1236.
13 A. Hellweg, S. A. Grün and C. Hättig, *Phys. Chem. Chem. Phys.*, 2008, **10**, 1.
14 N. O. C. Winter and C. Hättig, *J. Chem. Phys.*, 2011, **134**, 184101.
15 N. O. C. Winter and C. Hättig, *Chem. Phys.*, 2012, **401**, 217.
16 A. D. Becke, *J. Chem. Phys.*, 1993, **98**, 5648–5652.
17 A. Dreuw and M. Head-Gordon, *Chem. Rev.*, 2005, **105**, 4009.
18 D. Jacquemin, V. Wathelet, E. A. Perpète and C. Adamo, *J. Chem. Theory Comput.*, 2009, **5**, 2420–2435.
19 M. R. Silva-Junior, M. Schreiber, S. P. A. Sauer and W. Thiel, *J. Chem. Phys.*, 2010, **133**, 174318.
20 H. H. Falden, K. R. Falster-Hansen, K. L. Bak, S. Rettrup and S. P. A. Sauer, *J. Phys. Chem. A*, 2009, **113**, 11995–12012.
21 J. Fabian, *Theor. Chem. Acc.*, 2001, **106**, 199–217.
22 J. Fabian, L. A. Diaz, G. Seifert and T. Niehaus, *J. Mol. Struct.*, 2002, **594**, 41–53.
23 D. Jacquemin, E. A. Perpète, O. A. Vydrov, G. E. Scuseria and C. Adamo, *J. Chem. Phys.*, 2007, **127**, 094102.
24 D. Jacquemin, E. A. Perpète, G. E. Scuseria, I. Ciofini and C. Adamo, *J. Chem. Theory Comput.*, 2008, **4**, 123–135.
25 L. Goerigk and S. Grimme, *J. Chem. Phys.*, 2010, **132**, 184103.
26 R. Send, M. Kühn and F. Furche, *J. Chem. Theory Comput.*, 2011, **7**, 2376–2386.
27 A. Schäfer, C. Huber and R. Ahlrichs, *J. Chem. Phys.*, 1994, **100**, 5829.
28 F. Weigend, M. Häser, H. Patzelt and R. Ahlrichs, *Chem. Phys. Lett.*, 1998, **294**, 143.
29 T. H. Dunning, *J. Chem. Phys.*, 1989, **90**, 1007.
30 R. A. Kendall, T. H. Dunning and R. J. Harrison, *J. Chem. Phys.*, 1992, **96**, 6796–6806.
31 A development of University of Karlsruhe and Forschungszentrum Karlsruhe GmbH, 1989–2007, Turbomole GmbH, since 2007; available from http://www.turbomole.com, *TURBOMOLE V6.3*, 2011.
32 R. Bauernschmitt and R. Ahlrichs, *Chem. Phys. Lett.*, 1996, **256**, 454–464.
33 F. Furche and R. Ahlrichs, *J. Chem. Phys.*, 2002, **117**, 7433–7447.
34 F. Weigend, A. Köhn and C. Hättig, *J. Chem. Phys.*, 2002, **116**, 3175.
35 T. V. Nguyen and D. W. Pratt, *J. Chem. Phys.*, 2006, **124**, 054317.
36 T. Bürgi and S. Leutwyler, *J. Chem. Phys.*, 1994, **101**, 8418.
37 U. Even, J. Magen, J. Jortner, J. Friedman and H. Levanon, *J. Chem. Phys.*, 1982, **77**, 4374–4383.
38 T. M. Dunn, R. Tembreull and D. M. Lubman, *Chem. Phys. Lett.*, 1985, **121**, 453.
39 E. Fujimaki, A. Fujii, T. Ebata and N. Mikami, *J. Chem. Phys.*, 1999, **110**, 4238.
40 R. S. Mulliken, *J. Chem. Phys.*, 1955, **23**, 1997.
41 J. Sepiol, Y. Stepanenko, A. Vdovin, A. Mordzinski, E. Vogel and J. Waluk, *Chem. Phys. Lett.*, 1998, **296**, 549–556.
42 U. Even, J. Magen and J. Jortner, *Chem. Phys. Lett.*, 1982, **88**, 131–134.
43 U. Even and J. Jortner, *J. Chem. Phys.*, 1982, **77**, 4391–4399.
44 U. Even and J. Jortner, *J. Chem. Phys.*, 1983, **78**, 3445–3454.
45 S. Leutwyler, *J. Chem. Phys.*, 1984, **81**, 5480–5493.
46 T. Troxler, R. Knochenmuss and S. Leutwyler, *Chem. Phys. Lett.*, 1989, **159**, 554–558.
47 J. T. Yi, L. Alvarez-Valtierra and D. W. Pratt, *J. Chem. Phys.*, 2006, **124**, 244302.
48 Y. Nosenko, A. Kyrychenko, R. P. Thummel, J. Waluk, B. Brutschy and J. Herbich, *Phys. Chem. Chem. Phys.*, 2007, **9**, 3276–3285.
49 J. R. Carney and T. S. Zwier, *J. Phys. Chem.*, 2000, **104**, 8677.
50 W. C. Bouwman, A. C. Jones, D. Phillips, P. Thibodeau, C. Friel and R. L. Christensen, *J. Phys. Chem.*, 1990, **94**, 7429–7434.
51 E. A. El-Hakam, A. El-Nasr, A. Fujii, T. Yahagi, T. Ebata and N. Mikami, *J. Phys. Chem. A*, 2005, **109**, 2498–2504.
52 P. W. Joireman, R. T. Kroemer, D. W. Pratt and J. P. Simons, *J. Chem. Phys.*, 1996, **105**, 6075–6077.
53 J. R. Johnson, K. D. Jordan, D. F. Plusquellic and D. W. Pratt, *J. Chem. Phys.*, 1990, **93**, 2258–2273.
54 Y. Matsumoto, T. Ebata and N. Mikami, *J. Chem. Phys.*, 1998, **109**, 6303–6311.
55 Y. Matsumoto, T. Ebata and N. Mikami, *Chem. Phys. Lett.*, 2001, **338**, 52–60.
56 M. R. Nimlos, D. F. Kelley and E. R. Bernstein, *J. Phys. Chem.*, 1987, **91**, 6610–6614.
57 J. T. Yi, J. W. Ribblett and D. W. Pratt, *J. Phys. Chem. A*, 2005, **109**, 9456–9464.
58 S. K. Kim and E. R. Bernstein, *J. Phys. Chem.*, 1990, **94**, 3531–3539.
59 J. W. Ribblett, D. R. Borst and D. W. Pratt, *J. Chem. Phys.*, 1999, **111**, 8454.
60 D. R. Borst, D. W. Pratt and M. Schäfer, *Phys. Chem. Chem. Phys.*, 2007, **9**, 4563–4571.
61 T. M. Korter, D. R. Borst, C. J. Butler and D. W. Pratt, *J. Am. Chem. Soc.*, 2001, **123**, 96–99.
62 V. Venkatesan, A. Fujii, T. Ebata and N. Mikami, *J. Phys. Chem. A*, 2005, **109**, 915–921.
63 Y. Nibu, C. Okabe and H. Shimada, *J. Phys. Chem. A*, 2003, **107**, 1945–1954.
64 Y. Nibu, R. Marui and H. Shimada, *J. Phys. Chem. A*, 2006, **110**, 9627–9632.
65 Y. Matsuda, T. Ebata and N. Mikami, *J. Phys. Chem. A*, 2001, **105**, 3475–3480.
66 L. Alvarez-Valtierra, X.-Q. Tan and D. W. Pratt, *J. Phys. Chem. A*, 2007, **111**, 12802–12809.
67 A. Fujii, Y. Kitamura and N. Mikami, *J. Chem. Phys.*, 2000, **113**, 8000–8008.
68 A. Held, B. B. Champagne and D. W. Pratt, *J. Chem. Phys.*, 1991, **95**, 8732–8743.
69 E. Fujimaki, A. Fujii, T. Ebata and N. Mikami, *J. Chem. Phys.*, 2000, **112**, 137–148.
70 S. J. Humphrey and D. W. Pratt, *J. Chem. Phys.*, 1993, **99**, 5078–5086.
71 C. L. Janssen and I. M. B. Nielsen, *Chem. Phys. Lett.*, 1998, **290**, 423–430.
72 J. A. Frey, R. Leist, C. Tanner, H.-M. Frey and S. Leutwyler, *J. Chem. Phys.*, 2006, **125**, 114308.

 This journal is © the Owner Societies 2013